



This is a repository copy of *High-shear granulation : an investigation into granule breakage rates*.

White Rose Research Online URL for this paper:
<https://eprints.whiterose.ac.uk/176514/>

Version: Accepted Version

Article:

de Koster, S.A.L., liu, L.X., Litster, J. orcid.org/0000-0003-4614-3501 et al. (1 more author) (2021) High-shear granulation : an investigation into granule breakage rates. *Advanced Powder Technology*, 32 (5). pp. 1390-1398. ISSN 0921-8831

<https://doi.org/10.1016/j.apr.2021.03.006>

© 2021 The Society of Powder Technology Japan. This is an author produced version of a paper subsequently published in *Advanced Powder Technology*. Uploaded in accordance with the publisher's self-archiving policy. Article available under the terms of the CC-BY-NC-ND licence (<https://creativecommons.org/licenses/by-nc-nd/4.0/>).

Reuse

This article is distributed under the terms of the Creative Commons Attribution-NonCommercial-NoDerivs (CC BY-NC-ND) licence. This licence only allows you to download this work and share it with others as long as you credit the authors, but you can't change the article in any way or use it commercially. More information and the full terms of the licence here: <https://creativecommons.org/licenses/>

Takedown

If you consider content in White Rose Research Online to be in breach of UK law, please notify us by emailing eprints@whiterose.ac.uk including the URL of the record and the reason for the withdrawal request.



eprints@whiterose.ac.uk
<https://eprints.whiterose.ac.uk/>

High-Shear Granulation: An Investigation into Granule Breakage Rates

Stefan. A. L. de Koster^a, Lian. X. Liu^b, James. D. Litster^a, Rachel. M. Smith^{a*}

a: Department of Chemical and Biological Engineering, The University of Sheffield, Mappin Street, Sheffield, S1 3JD

b: Department of Chemical and Process Engineering, University of Surrey, Guildford, Surrey, GU2 7XH

*Corresponding author: Rachel Smith, email: rachel.smith@sheffield.ac.uk, tel: +44-1142228255

Abstract

Granule breakage is an important rate process in wet granulation that promotes product uniformity and controls product size and strength. In this work, a model to predict granule breakage is proposed and experimentally validated. The model assumes exponential of the surviving granules, dependent on a probability of breakage; a function of powder and binder properties, as well as operating parameters. Validation experiments were performed with a breakage-only granulator, filled with cohesive, non-granulating sand. Premade pellets made from lactose monohydrate and silicone oils were granulated at several impeller speeds, and the number of survivors was observed over time. The results revealed that the number of granules did indeed decay exponentially. It was found that the overall probability of breakage was inversely proportional to the capillary number. Moreover, the pore saturation played an important role in determining the probability of breakage, with higher pore saturations reducing breakage overall. A comparison with experimental data from literature revealed that the developed models agrees qualitatively with the experimental data, but is unable to fully capture the effect of powder properties and powder-binder interaction.

Keywords

Wet granulation, High-shear, Breakage, Modelling

1 Introduction

Granulation is defined as the formation of agglomerates by agitation of smaller particles [1]. Using such agglomerates offers many advantages over using the raw materials. For instance, the handling, metering and dosing are improved [2], and the risk of dust explosions is greatly reduced [3]. This method of size enlargement can be achieved in several ways. In wet granulation, particles are agglomerated by mixing with a liquid binder. Agitation can be achieved using various types of equipment including tumbling drums, fluidised beds, and high-shear mixers. Because the use of granulated materials is preferred over the use of powder, granulation is widely applied in industries that deal with powder materials, such as the pharmaceutical industry [4]. Despite the wide application of granulation and over 60 years of research [4], however, most mechanisms of granulation are poorly understood due to the complexity of the process [5]. This is true for high-shear granulation in particular [6].

Three key mechanisms are discerned in wet granulation: wetting and nucleation; consolidation and growth; and breakage and attrition [4]. These mechanisms describe the formation, growth and destruction of granules, respectively. Although wetting and nucleation and consolidation and growth are not fully understood, regime maps have been developed which help increase our understanding of these two phenomena [7-9]. For breakage and attrition, however, such tools are lacking, which makes it one of the least understood rate processes [5].

Although breakage and attrition is poorly understood, it is an important process, especially in high-shear wet granulation, where shear forces are more likely to damage granules compared to, for example, tumbling drums. Breakage promotes the distribution of liquid and homogeneity of the product, and can also be used for size and strength control [5, 10]. In order to predict

granulated product quality and resistance to wear during further processing and transport, it is important to understand breakage and attrition [5].

Vogel and Peukert [11] report an expression that describes the fracture of granules as a probability of breakage s , as defined in Equation 1:

$$s = 1 - \exp\left(-f_{Mat} * x * k * (W_{m,kin} - W_{m,min})\right) \quad (1)$$

where f_{Mat} is a material parameter defining fracture behaviour of the particle, x is the particle size, k is the impact number, $W_{m,kin}$ is the kinetic energy of the particle, and $W_{m,min}$ is the minimum kinetic energy required for particle breakage. Vogel and Peukert successfully used population balance modelling, incorporating this approach to model a lab-scale mill. Their findings imply that breakage is subject to probabilistic phenomena and can be described with statistics: depending on granule properties and the operating conditions of the equipment used, granules have varying probability to break.

Van den Dries et al. [12] first investigated the relationship between the breakage number of granules and the Stokes deformation number St_{def} , which describes the deformability of granules [8, 9, 13], for high-shear granulation, as shown in Equation 2.

$$St_{def} = \frac{\frac{1}{2} * \rho_g * v_c^2}{\sigma_p} \quad (2)$$

Here, ρ_g is the granule density, v_c is the granule impact velocity, σ_p is the dynamic yield stress of the granule. They found that at low Stokes deformation numbers, damage mostly occurred due to attrition. At and above a critical Stokes deformation number, full breakage occurred.

Liu et al. [14] and Smith et al. [15] further investigated the relationship between the Stokes deformation number and granule breakage by developing a breakage-only granulator (BOG). This granulator was filled with non-granulating sand, and a fixed number of pre-formed granules were added. Two different impellers were used: a two-bladed bevelled edge impeller, and a flat plate impeller. The number of broken granules was monitored over time and related to the Stokes deformation number. To estimate the dynamic yield stress, a theoretical formula was used, as shown by Equation 3:

$$\sigma_p = AR^{-4.3} * S * \left[6 * \frac{1 - \varepsilon}{\varepsilon} * \frac{\gamma * \cos(\theta)}{d_{3,2}} + \frac{9}{8} * \left(\frac{1 - \varepsilon}{\varepsilon} \right)^2 * \frac{9 * \pi * \mu * v_p}{16 * d_{3,2}} \right] \quad (3)$$

where AR is the shape factor of the primary particles, S is the liquid saturation of the granule, ε is the porosity of the granule, γ is the surface tension, θ is the powder-binder contact angle, $d_{3,2}$ is the primary particle Sauter mean diameter, μ is the binder viscosity. v_p is the relative granule velocity, which was assumed to be 15 % of the impeller tip speed. They employed the same breakage/no-breakage criterion to find a critical Stokes deformation number, below which no breakage occurs. This theory held for the bevelled edge impeller, but was mostly qualitative for the flat plate impeller. This difference was partly due to the fact that the particles tested were not exactly the same. Although this model was successful in predicting the breakage of granules subjected to the required shear force, the model does not take into account the chance that granules will actually experience the forces required for breakage. This may be the reason why the model cannot predict granule breakage behaviour with a flat plate impeller.

Akiti et al. [16] have used a breakage-only granulator to study the parameters relevant to breakage and attrition. The work identified increasing binder viscosity, decreasing primary particle size, viscosity of the medium and shear time as ways to reduce granule breakage and

attrition. Stronger granules were found to tend towards attrition rather than breakage, whereas full breakage was observed for weaker granules. Population balance studies were capable of predicting the effects of changes in binder viscosity, primary particle size, and shear time on granule breakage behaviour.

This work aims to use the concept of breakage probability to develop a useful model to predict breakage behaviour using physically relevant properties of the powder-binder system and operating parameters. The model is based on the random distribution of granules over a breakage and a no-breakage zone in a mixer granulator. Two key parameters are proposed: the ratio between the breakage zone and the overall granulator volume, which shows how likely it is that a granule is in the breakage zone; and the probability of breakage, which shows how likely it is that a granule will actually break. The developed model is related to the granule properties and the operating conditions and compared to experimental and literature data.

2 Model development

Based on the probability of breakage in Vogel and Peukert's work [11], we propose that a granule breakage a model should incorporate three different groups of parameters: the granulator operating parameters, the granulator shape, and the properties of the powder-binder system used.

In order to incorporate these parameters, the granulator is assumed to be composed of two different zones. Figure 1 shows this concept for a symmetric vertical mixer. In the no-breakage zone, breakage does not occur; the granules are assumed to have zero probability of breakage. In the breakage zone, there is a possibility for breakage to occur. This probability of breakage is a material property of the granule, referred to as s in this work. The relative fraction of the granulator occupied by the breakage zone is referred to as r . This parameter should be

dependent on the granulator type and the operating conditions. Assuming the granules are distributed evenly throughout the granulator, the surviving number of granules N after a single impact can then be defined as shown in Equation 4:

$$N = N_0 * (1 - (r * s)) \quad (4)$$

where N_0 is the initial number of granules. For multiple collision events n , this equation can be expanded to Equation 5:

$$\frac{N}{N_0} = (1 - (r * s))^n \quad (5)$$

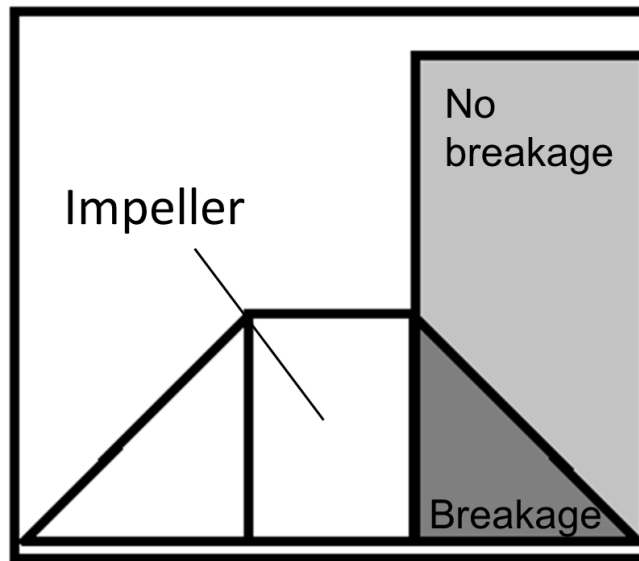


Figure 1: Schematic representation of a cross section of the granulator as considered by the model, with the breakage and no-breakage zone.

This equation predicts the fraction of intact granules after n impacts as a function of r and s . The number of impacts n is assumed to be a function of the impeller speed ω and the granulation time t , as well as the impeller shape factor f ($n = \omega * f * t$). This shape factor encodes the

number of collision events the granules experience for a single impeller revolution; for most impellers, the value can be assumed to be equal to the number of impeller blades, e.g. 3 for a three-bladed impeller. Where this is not the case, such as for flat-plate impellers, it should be possible to determine the shape factor experimentally.

By combining the logarithm rewrite rules $\exp(\ln(x)) = x$ and $\ln(x^a) = a * \ln(x)$, these assumptions allow Equation 5 to be rewritten into Equations 6 and 7:

$$\frac{N}{N_0} = \exp(\ln(1 - (r * s)) * \omega * f * t) \quad (6)$$

$$\frac{N}{N_0} = \exp(-a * t) \text{ with } a = -\ln(1 - (r * s)) * \omega * f \quad (7)$$

Here, a is a positive lumped parameter containing the experimental and operating parameters, as well as the granulator properties. This equation shows that the number of intact granules decays exponentially, which is in agreement with experimental investigations [17].

In this model, the most important parameters are the relative size of the breakage zone, r , and the probability of breakage s . The fraction of the breakage zone is most likely dependent on the granulator dimensions, operating speeds and powder-binder properties, which would affect the viscosity of the medium. It should be fairly straightforward to find this parameter by performing breakage experiments at different speeds, or by using an advanced technique like in-situ particle imaging. The most crucial parameter of the model is s . In the literature, several ways to calculate the probability of breakage have been proposed. We propose that the probability of breakage should be dependent on both the kinetic energy of the granules and the powder and binder properties.

2.1 Experimental

To evaluate the model and propose an expression for the combined term r^*s , breakage experiments were performed in a high shear mixer using granules made from lactose monohydrate and silicone oil according to the same procedure as described by Liu et al. [14]: Broad lactose ($D_{3,2} = 42.2 \mu\text{m}$) was kneaded in a plastic bag with silicone oil until the binder was evenly distributed. The mixture was then loaded into a cylindrical die with a diameter of 5 mm and a height of 5 mm and pressed into pellets of the same dimensions. Varying amounts of mixture were used to produce pellets with three different pore saturations: 0.3, 0.5 and 0.8.

Two different grades of silicone oil were used: 100 cSt and 1000 cSt, resulting in six different types of pellets overall. Each type of these pellets was introduced into a breakage-only granulator (BOG) [14]; a mixer granulator filled with cohesive sand. For each type of granule, the BOG was run at several speeds (750, 1000 and 1500 rpm) for 15 seconds. After a single experiment was finished, the granules were extracted and evaluated for breakage by passing the sand-granule mixture through a sieve. Any granules smaller than 3.38 mm were considered sufficiently damaged to be removed from further granulation. The surviving granules and the sand were then reintroduced into the BOG and the granulator was run for another 15 seconds. This procedure was repeated until no further survivors were obtained, or four successive sets of granulation had been performed. In this way, the number of surviving granules could be tracked over time. Using this method, a total of eighteen different data series were obtained, as shown in Table 1.

The obtained results were then compared to the proposed model and the parameter a and, consequently, parameter r^*s were obtained for each data set. Finally, the obtained parameters were related to dimensionless quantities to yield a way to predict granule breakage.

Table 1: Overview of the different validation experiments performed using the BOG for this study.

100 cSt silicone oil			1000 cSt silicone oil		
Sat = 0.3	Sat = 0.5	Sat = 0.8	Sat = 0.3	Sat = 0.5	St = 0.8
ω (rpm)	ω (rpm)	ω (rpm)	ω (rpm)	ω (rpm)	ω (rpm)
500	500	500	500	500	500
750	750	750	750	750	750
1000	1000	1000	1000	1000	1000

3 Results and Discussion

Figure 2 shows a comparison between the model developed in this work and the experimental data. The number of surviving granules is shown as a function of time, scaled by the fitted lumped parameter a . The figure clearly demonstrates that the surviving number of granules decays exponentially. Some data sets are clustered either at the beginning or at the end of the curve. For these data sets, no breakage at all or significant breakage occurred, respectively. It is relatively easy for such sets to follow the predicted curve, since a is simply required to be either large in the case of significant breakage or small in the case of no breakage to follow the model. Therefore, the sets towards the middle of the curve demonstrate better than other sets whether the proposed model describes breakage behaviour sufficiently; data sets in the intermediate range of $0.008 < a < 0.1 \text{ s}^{-1}$ are of particular interest. These sets are the 100 cSt silicone oil sets with 0.5 and 0.8 saturation at 1000 and 1500 rpm, as well as all 1000 cSt sets at 0.5 saturation.

- 100 cSt, 0.3 S, 750 RPM ● 100 cSt, 0.5 S, 750 RPM ● 100 cSt, 0.8 S, 750 RPM
- 100 cSt, 0.3 S, 1000 RPM ■ 100 cSt, 0.5 S, 1000 RPM ■ 100 cSt, 0.8 S, 1000 RPM
- ▲ 100 cSt, 0.3 S, 1500 RPM ▲ 100 cSt, 0.5 S, 1500 RPM ▲ 100 cSt, 0.8 S, 1500 RPM
- 1000 cSt, 0.3 S, 750 RPM ○ 1000 cSt, 0.5 S, 750 RPM ○ 1000 cSt, 0.8 S, 750 RPM
- 1000 cSt, 0.3 S, 1000 RPM □ 1000 cSt, 0.5 S, 1000 RPM □ 1000 cSt, 0.8 S, 1000 RPM
- △ 1000 cSt, 0.3 S, 1500 RPM △ 1000 cSt, 0.5 S, 1500 RPM △ 1000 cSt, 0.8 S, 1500 RPM

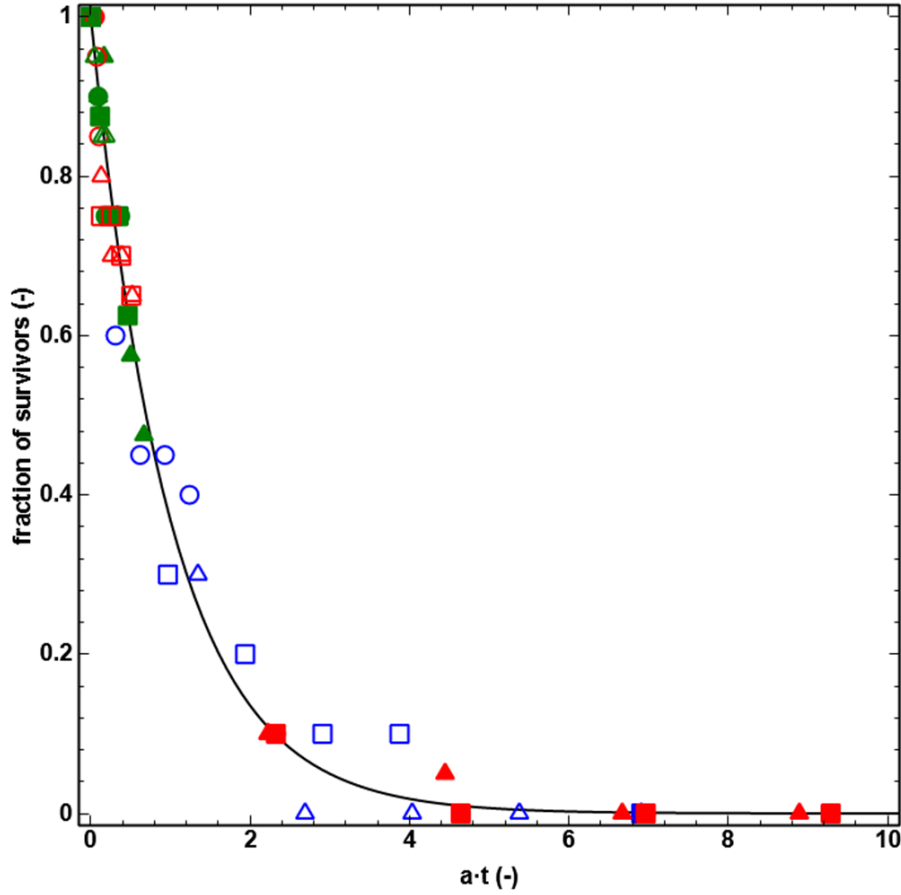


Figure 2: Fraction of surviving granules as a function of $a*t$. All curves collapse onto the single curve e^{-t} .

By fitting the lumped parameter a to the experimental data, it was possible to determine the fitted values for $r*s$ using Equation 7. The key challenge then was to link the relevant parameters to the obtained values to determine the physical phenomena governing breakage rates. Three potential candidates have been investigated in this work.

The first option is the Stokes deformation number St_{def} . This number has been shown to be related to granule breakage in the literature [14]. The granule impact velocity was assumed to

be 15 % of the impeller tip speed, a value that was found to be representative for typical granule velocities in the type of granulator used [14]. Since a two-bladed impeller was used, the shape factor f was assumed to be 2.

The second option for correlation with the probability of breakage is the dimensionless peak flow stress Str^* , which represents the strength of a granule (Equation 8).

$$Str^* = \frac{\sigma_p * d_{3,2}}{\gamma * \cos(\theta)} \quad (8)$$

Here, all parameters are as defined in Equation 3, which was also used to approximate σ_p .

Finally, the capillary number Ca is a possible candidate for correlation with breakage, as it is known to be related to Str^* [18-20] (Equation 9):

$$Ca = \frac{\mu * v_p}{\gamma * \cos(\theta)} \quad (9)$$

Again, all parameters in this equation are as defined in Equation 3.

3.1 Correlation of breakage to the Stokes deformation number

Using Equations 2 and 3, the theoretical Stokes deformation number was calculated for all evaluated granule sets. Figure 3 shows the overall probability of breakage r^* s as a function of the Stokes deformation number. As the Stokes deformation number increases, so does the overall probability of breakage. This is logical, as an increased Stokes deformation number indicates weaker, more deformable granules. However, there does not appear to be a direct correlation between the Stokes deformation number and the overall probability of breakage.

- 100 cSt, 0.3 S, 750 RPM ● 100 cSt, 0.5 S, 750 RPM ● 100 cSt, 0.8 S, 750 RPM
- 100 cSt, 0.3 S, 1000 RPM ■ 100 cSt, 0.5 S, 1000 RPM ■ 100 cSt, 0.8 S, 1000 RPM
- ▲ 100 cSt, 0.3 S, 1500 RPM ▲ 100 cSt, 0.5 S, 1500 RPM ▲ 100 cSt, 0.8 S, 1500 RPM
- 1000 cSt, 0.3 S, 750 RPM ○ 1000 cSt, 0.5 S, 750 RPM ○ 1000 cSt, 0.8 S, 750 RPM
- 1000 cSt, 0.3 S, 1000 RPM □ 1000 cSt, 0.5 S, 1000 RPM □ 1000 cSt, 0.8 S, 1000 RPM
- △ 1000 cSt, 0.3 S, 1500 RPM △ 1000 cSt, 0.5 S, 1500 RPM △ 1000 cSt, 0.8 S, 1500 RPM

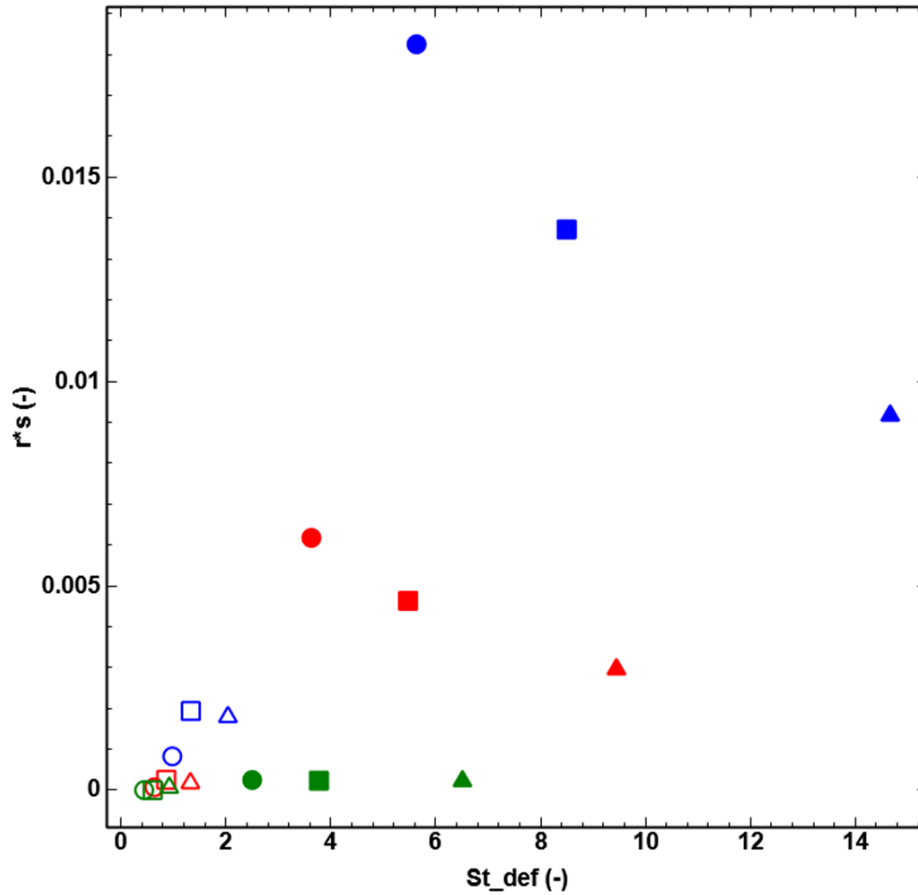


Figure 3: The overall probability of breakage r^*s plotted against the Stokes deformation number St_{def} .

Some general trends are visible, e.g. the probability of breakage tends to go down with an increase in binder viscosity. Additionally, an increase in liquid saturation also results in a decrease in granule breakage. Finally, the probability of breakage goes down with an increase in St_{def} . However, the relationship between r^*s and St_{def} is unclear; there appears to be no direct correlation. This behaviour is likely caused by the assumptions used when calculating the granule dynamic strength (Equation 3) and the Stokes deformation number (Equation 2). It is

assumed that both the relative granule velocity, v_p , and the granule impact velocity, v_c , are equal to 15% of the impeller speed. Any changes in the ratio between these two velocities will result in different values for St_{def} . Therefore, if a slightly different ratio were to be assumed, the observed trend of r^*s versus St_{def} would be different from what is presented in Figure 3. As such, the trend in Figure 3 may be more an artefact than the real situation. Due to the uncertainties in calculating St_{def} using the current assumptions for granule velocity, no conclusions can be drawn on the relationship between r^*s and St_{def} .

3.2 Correlation of breakage to the dimensionless peak flow stress

The dimensionless peak flow stress was calculated using Equations 3 and 8. Since breakage was expected to decrease with increasing granule strength, the *inverse* of the dimensionless peak flow stress was used for correlation with the overall probability of breakage r^*s . Figure 4 clearly shows that a decrease in the dimensionless peak flow stress results in an increase in the probability of breakage. It appears as though two regimes are present; a regime with little correlation, and a regime with a stronger, linear correlation. It should be noted here that the low saturation, low viscosity samples (100 cSt; 0.3 saturation) appear the most linear, but actually contribute little to inferring any trends from the data; these sets have a very high probability of breakage and will as such always be predicted well. The sets that do not contribute to the model are the three sets with 100 cSt silicone oil and 0.3 saturation, and the sets with 1000 cSt silicone oil, 0.8 saturation at 750 and 1500 rpm. These sets have been omitted for fitting.

- 100 cSt, 0.3 S, 750 RPM ● 100 cSt, 0.5 S, 750 RPM ● 100 cSt, 0.8 S, 750 RPM
- 100 cSt, 0.3 S, 1000 RPM ■ 100 cSt, 0.5 S, 1000 RPM ■ 100 cSt, 0.8 S, 1000 RPM
- ▲ 100 cSt, 0.3 S, 1500 RPM ▲ 100 cSt, 0.5 S, 1500 RPM ▲ 100 cSt, 0.8 S, 1500 RPM
- 1000 cSt, 0.3 S, 750 RPM ○ 1000 cSt, 0.5 S, 750 RPM ○ 1000 cSt, 0.8 S, 750 RPM
- 1000 cSt, 0.3 S, 1000 RPM □ 1000 cSt, 0.5 S, 1000 RPM □ 1000 cSt, 0.8 S, 1000 RPM
- △ 1000 cSt, 0.3 S, 1500 RPM △ 1000 cSt, 0.5 S, 1500 RPM △ 1000 cSt, 0.8 S, 1500 RPM

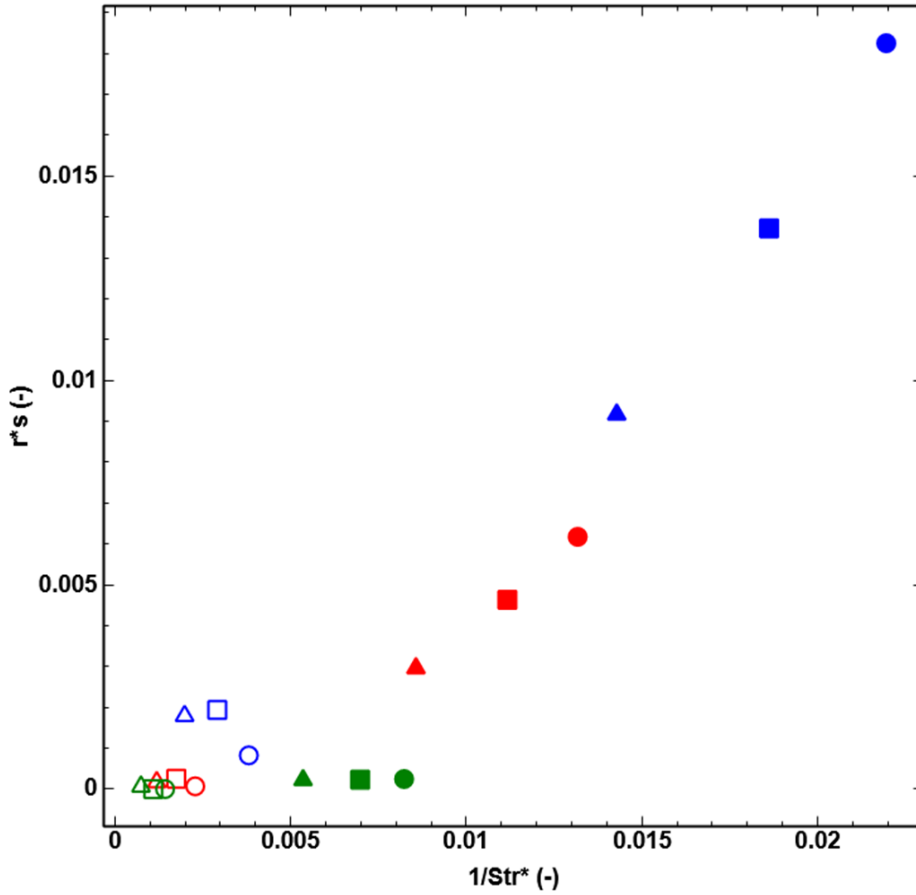


Figure 4: The overall probability of breakage $r*s$ plotted against the inverse of the dimensionless peak flow stress Str^* .

Using Python's `curve_fit` method, it was found that both r and s could be predicted according to Equation 10:

$$s = \frac{c_1}{Str^*} + c_2 \text{ with } r = \omega * c_3 \quad (10)$$

with c_1 and c_2 dimensionless fitting constants. It is likely that the size of the breakage zone is related to the impeller speed. In Equation 10, it is assumed that r is directly related to the impeller speed ω by constant c_3 , which equals 0.00155 s. For the first regime, it was found that c_1 equals 4.05 with c_2 set to 0; for the second regime, c_1 equals 56.7 and c_2 equals -0.436 (the intersect being at $Str^* = 121$). The resulting line is shown in Figure 5.

- 100 cSt, 0.3 S, 750 RPM ● 100 cSt, 0.5 S, 750 RPM ● 100 cSt, 0.8 S, 750 RPM
- 100 cSt, 0.3 S, 1000 RPM ■ 100 cSt, 0.5 S, 1000 RPM ■ 100 cSt, 0.8 S, 1000 RPM
- ▲ 100 cSt, 0.3 S, 1500 RPM ▲ 100 cSt, 0.5 S, 1500 RPM ▲ 100 cSt, 0.8 S, 1500 RPM
- 1000 cSt, 0.3 S, 750 RPM ○ 1000 cSt, 0.5 S, 750 RPM ○ 1000 cSt, 0.8 S, 750 RPM
- 1000 cSt, 0.3 S, 1000 RPM □ 1000 cSt, 0.5 S, 1000 RPM □ 1000 cSt, 0.8 S, 1000 RPM
- △ 1000 cSt, 0.3 S, 1500 RPM △ 1000 cSt, 0.5 S, 1500 RPM △ 1000 cSt, 0.8 S, 1500 RPM

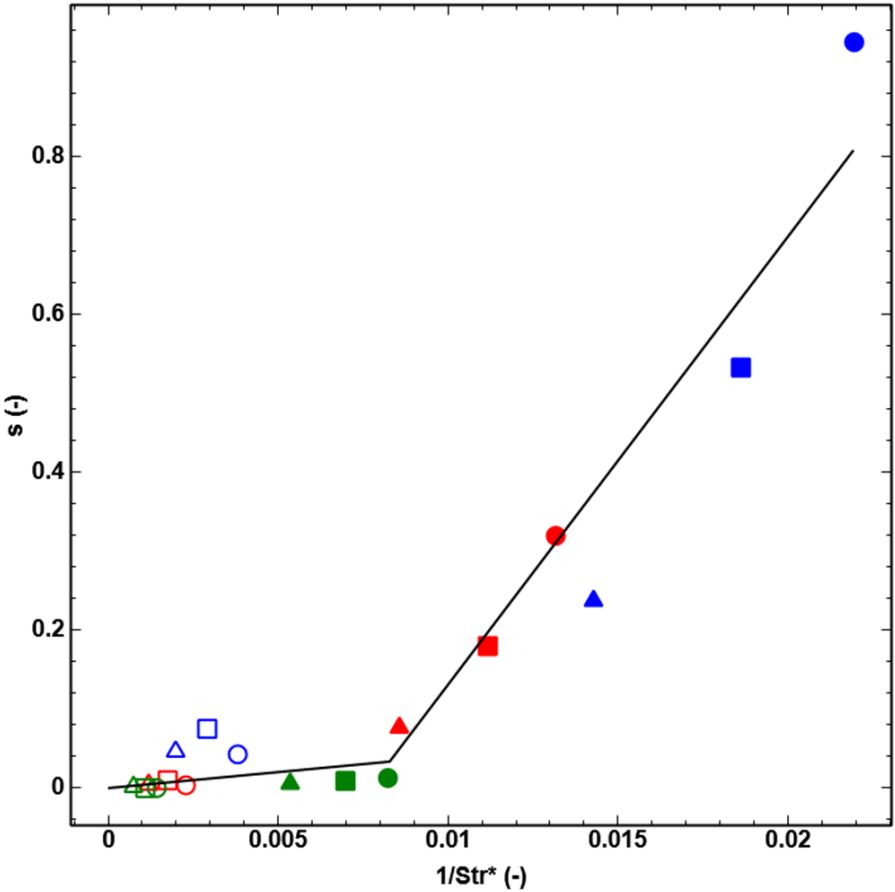


Figure 5: The probability of breakage s plotted against the inverse of the dimensionless peak flow stress Str^* with fit.

Figure 5 appears to yield a good fit of most values. The low saturation, high viscosity sets appear to deviate slightly from the overall trend, but overall, the fit seems satisfactory. However, as Figure 6 demonstrates, using the obtained relationship to predict values of lumped parameter a , does not yield a good fit for most data sets.

- 100 cSt, 0.3 S, 750 RPM ● 100 cSt, 0.5 S, 750 RPM ● 100 cSt, 0.8 S, 750 RPM
- 100 cSt, 0.3 S, 1000 RPM ■ 100 cSt, 0.5 S, 1000 RPM ■ 100 cSt, 0.8 S, 1000 RPM
- ▲ 100 cSt, 0.3 S, 1500 RPM ▲ 100 cSt, 0.5 S, 1500 RPM ▲ 100 cSt, 0.8 S, 1500 RPM
- 1000 cSt, 0.3 S, 750 RPM ○ 1000 cSt, 0.5 S, 750 RPM ○ 1000 cSt, 0.8 S, 750 RPM
- 1000 cSt, 0.3 S, 1000 RPM □ 1000 cSt, 0.5 S, 1000 RPM □ 1000 cSt, 0.8 S, 1000 RPM
- △ 1000 cSt, 0.3 S, 1500 RPM △ 1000 cSt, 0.5 S, 1500 RPM △ 1000 cSt, 0.8 S, 1500 RPM

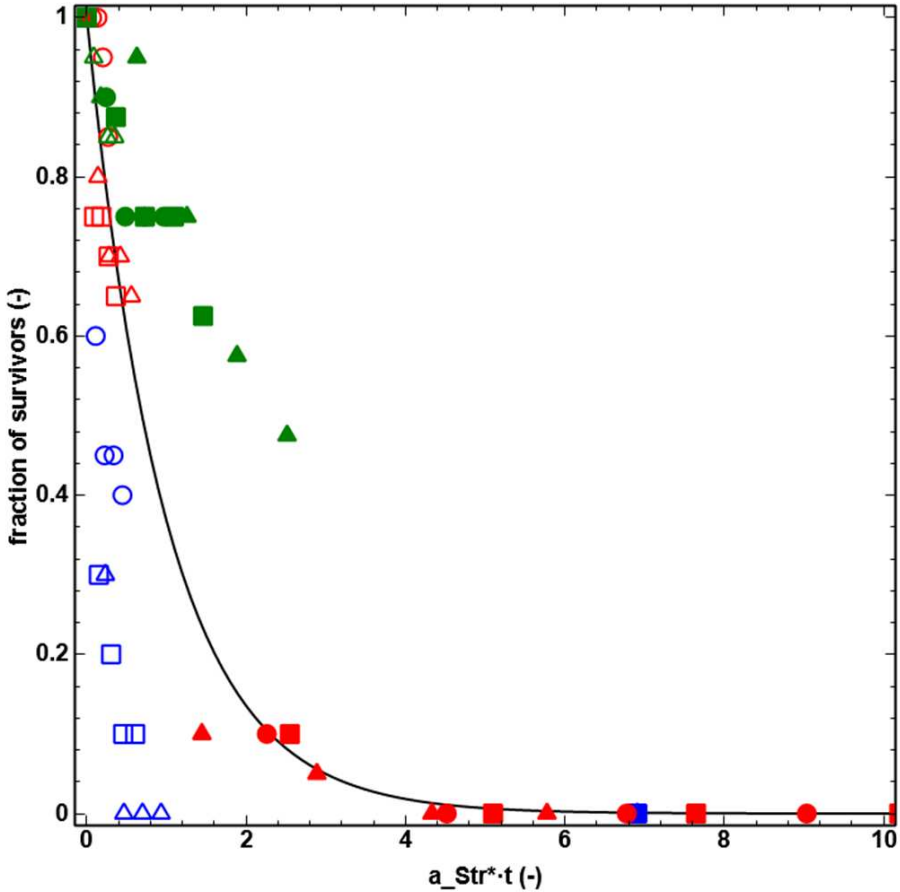


Figure 6: Fraction of surviving granules as a function of time, scaled with the estimated fitting parameter a_{Str^*} . Theoretically, all data should collapse onto a single curve.

Sets with medium saturation (0.5) are fairly well predicted, but sets with both high and low saturation values are very poorly predicted. The exponential factor exacerbates relatively small errors from the fit in Equation 11. Furthermore, all reasonably well predicted behaviour can be ascribed to data sets that show either little or extensive breakage. As such, this behaviour is easier to approximate well. From these observations, it can be concluded that the dimensionless peak flow stress does not sufficiently describe the observed breakage behaviour.

3.3 Correlation of breakage to the capillary number

The capillary number was calculated using Equation 9. In the literature the capillary number is often related to the dimensionless peak flow stress using two regimes, a static regime and an viscosity-dominated regime, as described by Equation 11 [18-20]:

$$Str^* = k_1 + k_2 * Ca^n \quad (11)$$

Here, k_1 and k_2 are constants describing the static strength of the granules and the location of the transition from the static regime to the viscosity-dominated regime, respectively, and n is the exponent, which usually has a value of approximately 0.5 in the literature [19, 20].

Since breakage generally involves relatively high shear rates, it is reasonable to assume that the capillary number can be related to the dimensionless peak flow stress according to the viscosity-dominated regime. Therefore, the *inverse* of the capillary number was used for correlation with the overall probability of breakage. Two observations can be made from this comparison, which is shown in Figure 7.

First of all, an increase in the capillary number leads to a decrease in the probability of breakage. This is logical, as an increase in the viscous forces, either by an increase in the granule velocity

or binder viscosity, should increase granule strength. Second, it appears as though there is a linear relationship between the inverse capillary number and the probability of breakage, provided the pore saturation remains constant. However, the pore saturation itself appears to have a separate effect on the probability of breakage as well; an increase in pore saturation results in a decrease in breakage. This is in agreement with Equation 3; granules with a higher pore saturation should have a higher strength.

- 100 cSt, 0.3 S, 750 RPM ● 100 cSt, 0.5 S, 750 RPM ● 100 cSt, 0.8 S, 750 RPM
- 100 cSt, 0.3 S, 1000 RPM ■ 100 cSt, 0.5 S, 1000 RPM ■ 100 cSt, 0.8 S, 1000 RPM
- ▲ 100 cSt, 0.3 S, 1500 RPM ▲ 100 cSt, 0.5 S, 1500 RPM ▲ 100 cSt, 0.8 S, 1500 RPM
- 1000 cSt, 0.3 S, 750 RPM ○ 1000 cSt, 0.5 S, 750 RPM ○ 1000 cSt, 0.8 S, 750 RPM
- 1000 cSt, 0.3 S, 1000 RPM □ 1000 cSt, 0.5 S, 1000 RPM □ 1000 cSt, 0.8 S, 1000 RPM
- △ 1000 cSt, 0.3 S, 1500 RPM △ 1000 cSt, 0.5 S, 1500 RPM △ 1000 cSt, 0.8 S, 1500 RPM

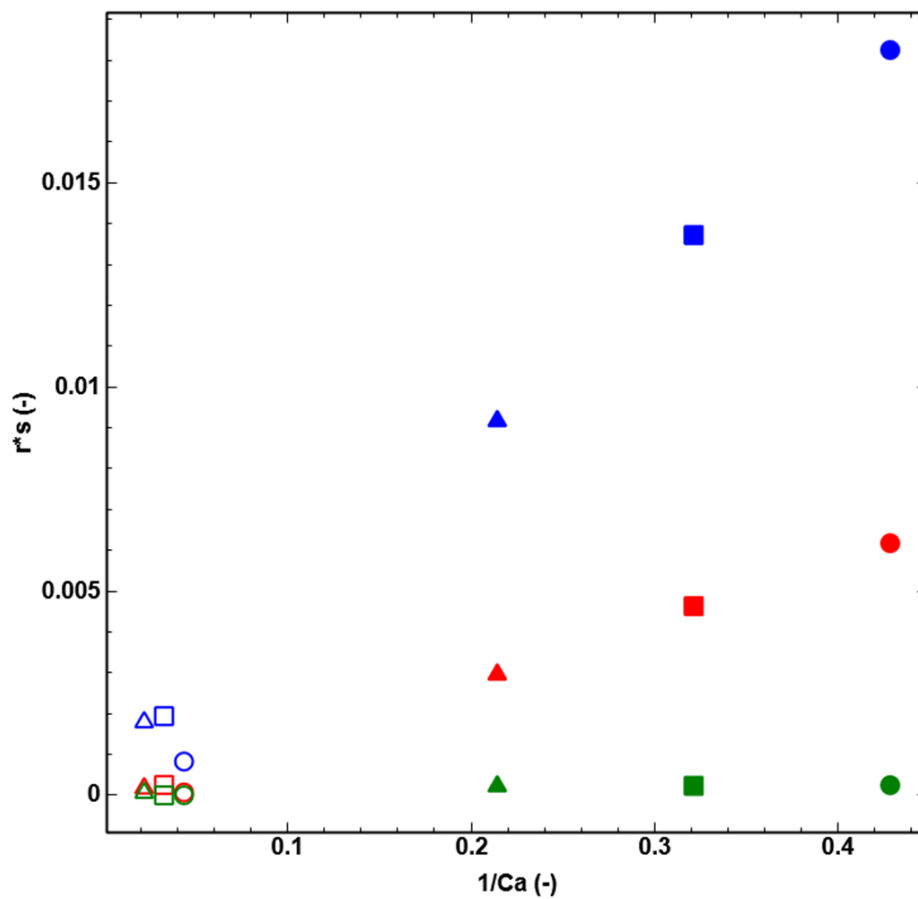


Figure 7: The overall probability of breakage r^*s plotted against the inverse of the capillary number Ca .

Further investigation into the effect of the pore saturation on the correlation between the inverse capillary number and the overall probability of breakage using *curve_fit* in Python reveals the following relationship (Equation 12):

$$r * s = \frac{\exp(-8.68 * S)}{Ca} \quad (12)$$

where, all parameters are as defined before. This equation is not perfect; it is highly likely that it lumps together the effect of changes in the relative size of the breakage zone described by r , which is affected by impeller speed, type, fill level and granulator shape, and the actual probability of breakage s . However, the equation is a good starting point for the prediction of granule breakage. It should also be noted that this equation is most likely only valid for viscosity-dominated strength behaviour. The only parameters investigated for the capillary number are changes in the liquid viscosity and the impeller speed, as the silicone oils used have similar contact angles and surface tensions.

All parameters required for the equation are relatively easy to determine granule properties: pore saturation, binder viscosity and surface tension, and the powder-binder contact angle. The only parameter that is challenging to obtain is the granule velocity. However, assuming the granule velocity scales linearly with the impeller tip speed, this should only affect the Capillary number.

It should be noted that the obtained fitting parameter of 8.68 for the correlation between the inverse capillary number and the overall probability of breakage could be dependent on other parameters. In this study, only lactose-silicone oil systems were evaluated. It is quite possible that the obtained parameter changes when using different powders and binders. A wider range of powders and binders must be investigated to verify this.

Substituting Equation 12 into Equation 7 yields the following expression to predict the surviving number of granules as a function of time (Equation 13):

$$\frac{N}{N_0} = \exp\left(\ln\left(1 - \left(\frac{\exp(-8.68 * S)}{Ca}\right)\right) * \omega * f * t\right) \quad (13)$$

Using this equation, the lumped parameter a_{Ca} was predicted for each data set evaluated and compared to the predicted model, as shown in Figure 8. Compared to Figure 6, Figure 8 shows a much better agreement between model and experimental data. Most breakage behaviour is predicted quite well by Equation 12, with the 1000 cSt, 0.3 saturation, 750 RPM set showing the most significant deviations in the $0.008 < a < 0.1 \text{ s}^{-1}$ range. It is possible that this data set is an outlier, but further experiments are needed to provide conclusive evidence.

- 100 cSt, 0.3 S, 750 RPM ● 100 cSt, 0.5 S, 750 RPM ● 100 cSt, 0.8 S, 750 RPM
- 100 cSt, 0.3 S, 1000 RPM ■ 100 cSt, 0.5 S, 1000 RPM ■ 100 cSt, 0.8 S, 1000 RPM
- ▲ 100 cSt, 0.3 S, 1500 RPM ▲ 100 cSt, 0.5 S, 1500 RPM ▲ 100 cSt, 0.8 S, 1500 RPM
- 1000 cSt, 0.3 S, 750 RPM ○ 1000 cSt, 0.5 S, 750 RPM ○ 1000 cSt, 0.8 S, 750 RPM
- 1000 cSt, 0.3 S, 1000 RPM □ 1000 cSt, 0.5 S, 1000 RPM □ 1000 cSt, 0.8 S, 1000 RPM
- △ 1000 cSt, 0.3 S, 1500 RPM △ 1000 cSt, 0.5 S, 1500 RPM △ 1000 cSt, 0.8 S, 1500 RPM

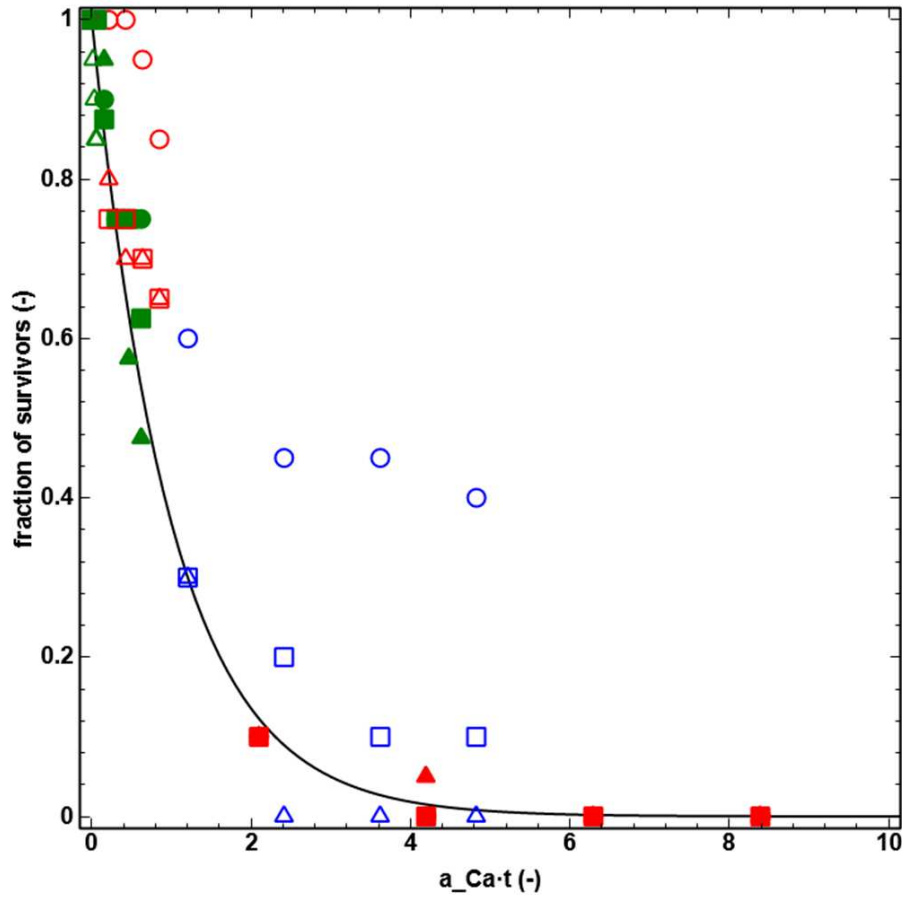


Figure 8: Fraction of surviving granules as a function of time, scaled with the estimated fitting parameter a_{Ca} . Theoretically, all data should collapse onto the black curve e^{-t} .

3.4 Comparison with data from the literature

In order to test the validity of the relationship proposed in Equation 12, experimental data from work performed by Suhairi [21] was used with permission from the authors. The data comprises four different systems: lactose-silicone oil, glass beads-silicone oil, lactose-water and glass beads-water. Granules were prepared similarly to the granules prepared in this work, and

various liquid saturations (0.3, 0.5, 0.6, 0.8, 1.0) were used. The largest difference in the experimental method was the extraction method; extracted intact granules were not reintroduced into the granulator. Instead, a fresh batch of granules was introduced into the granulator for a longer granulation time. Using this method, it was possible for the number, of survivors to increase between batches, which led to slightly more erratic data (particularly lactose-silicone oil at 0.5, 0.8 and 1.0 S), as shown in Figure 9.

- Glass-Silicone oil, 0.3 S
- Glass-Silicone oil, 0.5 S
- ▲ Glass-Silicone oil, 0.6 S
- ▼ Glass-Silicone oil, 0.8 S
- ◆ Glass-Silicone oil, 1.0 S
- Glass-Water, 0.3 S
- Glass-Water, 0.5 S
- △ Glass-Water, 0.6 S
- ▽ Glass-Water, 0.8 S
- ◇ Glass-Water, 1.0 S
- Lactose-Silicone oil, 0.3 S
- Lactose-Silicone oil, 0.5 S
- ▲ Lactose-Silicone oil, 0.6 S
- ▼ Lactose-Silicone oil, 0.8 S
- ◆ Lactose-Silicone oil, 1.0 S
- Lactose-Water, 0.3 S
- Lactose-Water, 0.5 S
- △ Lactose-Water, 0.6 S

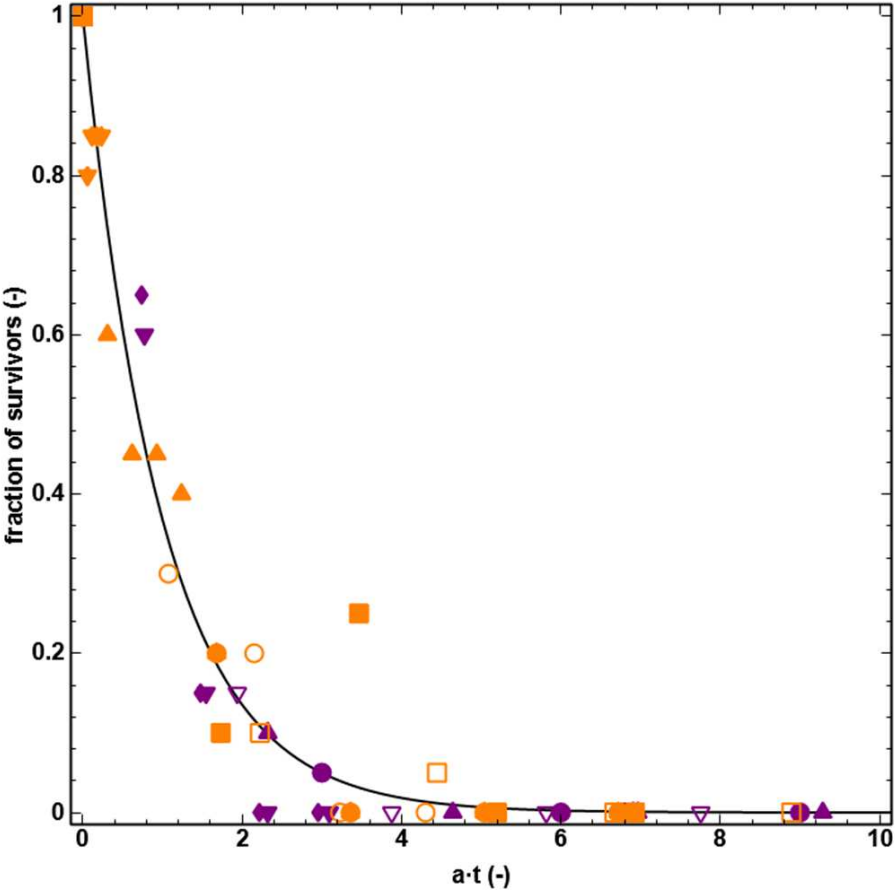


Figure 9: Fraction of surviving granules from the literature data set as a function of a^*t . Theoretically, all data should collapse onto the black curve e^{-a^*t} . Data shown was used with permission from the authors [21].

Although the proposed breakage trend still holds for this data set, the values in Figure 9 deviate more from the exponential decay curve. This can mostly be attributed to the experimental set-up; in some cases the surviving number of granules *increases*, which would not be possible with the set-up used in our study. Another potential issue is the dissolution of lactose for the lactose-water systems, which was observed by the authors. It should also be noted that most sets produced with water or glass beads showed significant breakage after even 15 s of granulation, essentially contributing nothing to the theory proposed here. For these systems, a shorter granulation time is needed to properly investigate the breakage behaviour.

Despite these caveats, the data sets provides more values for pore saturation, as well as the opportunity to investigate the effect of powder size and shape and powder-binder interaction to test the relationship found in Equation 12. Figure 10 shows a comparison between the observed values for r^*s and the values predicted using Equation 12 for the experimental data set as well as the test set from literature. In the case of a perfect prediction, the data points should fall on the black line.

From Figure 10, it becomes clear that the r^*s -values is much poorer compared to the values obtained for the experimental set; up to three orders of magnitude difference may be observed for some values. In particular, the predicted probability of breakage for systems with water as a binder is much higher than observed, and silicone-based systems have a higher probability of breakage than predicted.

- 100 cSt, 0.3 S, 750 RPM
- 100 cSt, 0.3 S, 1000 RPM
- ▲ 100 cSt, 0.3 S, 1500 RPM
- 100 cSt, 0.5 S, 750 RPM
- 100 cSt, 0.5 S, 1000 RPM
- ▲ 100 cSt, 0.5 S, 1500 RPM
- 100 cSt, 0.8 S, 750 RPM
- 100 cSt, 0.8 S, 1000 RPM
- ▲ 100 cSt, 0.8 S, 1500 RPM
- 1000 cSt, 0.3 S, 750 RPM
- 1000 cSt, 0.3 S, 1000 RPM
- △ 1000 cSt, 0.3 S, 1500 RPM
- 1000 cSt, 0.5 S, 750 RPM
- 1000 cSt, 0.5 S, 1000 RPM
- △ 1000 cSt, 0.5 S, 1500 RPM
- 1000 cSt, 0.8 S, 750 RPM
- 1000 cSt, 0.8 S, 1000 RPM
- △ 1000 cSt, 0.8 S, 1500 RPM
- Glass-Silicone oil, 0.3 S
- Glass-Silicone oil, 0.5 S
- ▲ Glass-Silicone oil, 0.6 S
- Glass-Silicone oil, 0.8 S
- Glass-Silicone oil, 1.0 S
- Glass-Water, 0.3 S
- Glass-Water, 0.5 S
- △ Glass-Water, 0.6 S
- ▽ Glass-Water, 0.8 S
- ◇ Glass-Water, 1.0 S
- Lactose-Silicone oil, 0.3 S
- Lactose-Silicone oil, 0.5 S
- ▲ Lactose-Silicone oil, 0.6 S
- ▽ Lactose-Silicone oil, 0.8 S
- ◇ Lactose-Silicone oil, 1.0 S
- Lactose-Water, 0.3 S
- Lactose-Water, 0.5 S
- △ Lactose-Water, 0.6 S

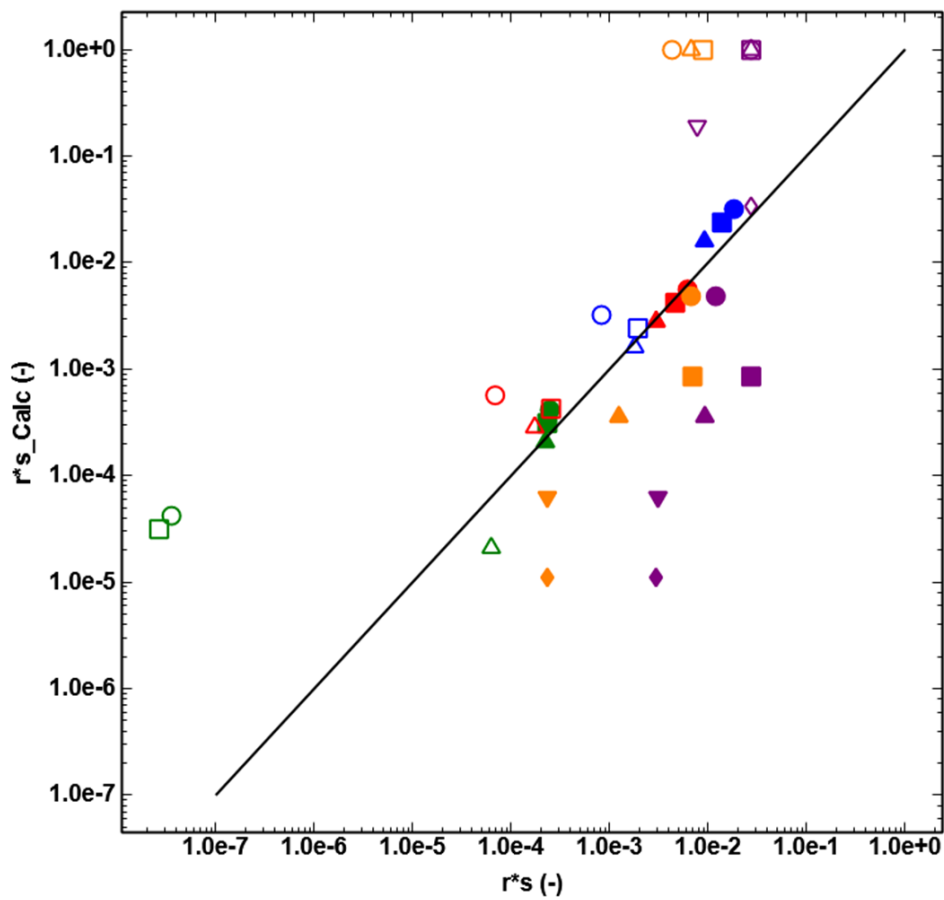


Figure 10: Comparison of the observed values for r^*s to the values predicted by Equation 12 for the experimental data sets presented in this work, as well as the literature data sets from Suhairi [21].

The values closest to the predictions are for systems using lactose and silicone oil; the powder and binder for the experimental data set. This observation suggests that powder and binder properties may play a more important role than assumed in Equation 12. Figure 11, which

shows the predicted breakage behaviour for the tests systems, confirms that Equation 12 does not encompass all phenomena involved in breakage.

- Glass-Silicone oil, 0.3 S
- Glass-Silicone oil, 0.5 S
- ▲ Glass-Silicone oil, 0.6 S
- ▼ Glass-Silicone oil, 0.8 S
- ◆ Glass-Silicone oil, 1.0 S
- Glass-Water, 0.3 S
- Glass-Water, 0.5 S
- △ Glass-Water, 0.6 S
- ▽ Glass-Water, 0.8 S
- ◇ Glass-Water, 1.0 S
- Lactose-Silicone oil, 0.3 S
- Lactose-Silicone oil, 0.5 S
- ▲ Lactose-Silicone oil, 0.6 S
- ▼ Lactose-Silicone oil, 0.8 S
- ◆ Lactose-Silicone oil, 1.0 S
- Lactose-Water, 0.3 S
- Lactose-Water, 0.5 S
- △ Lactose-Water, 0.6 S

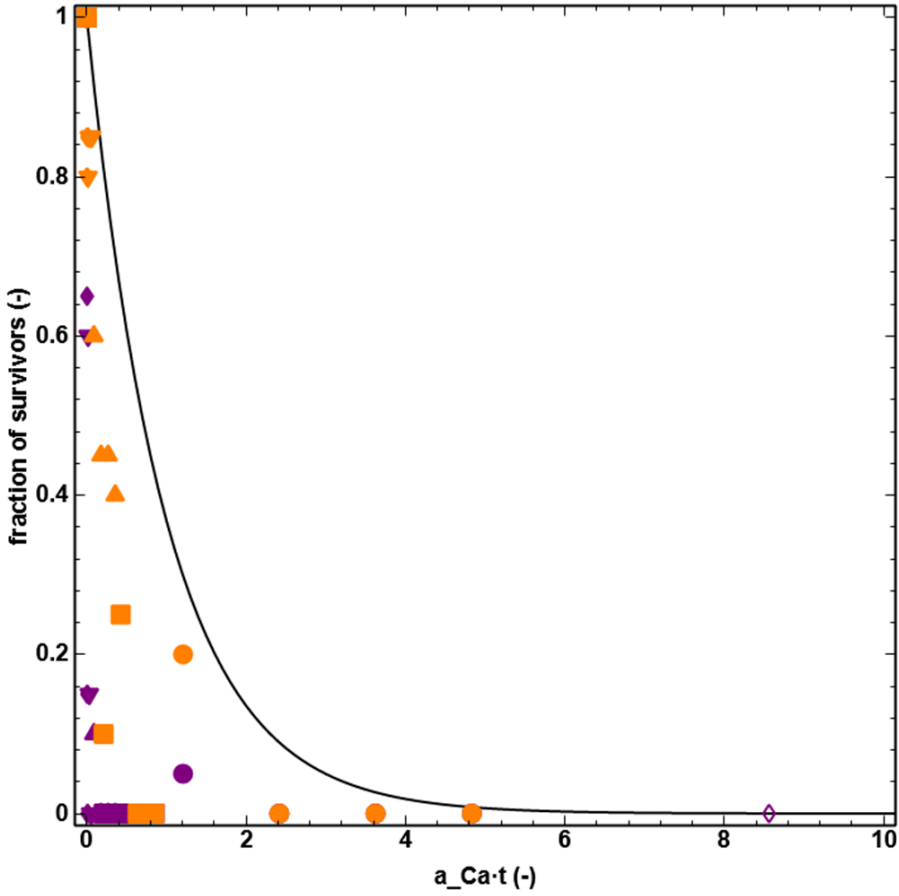


Figure 11: Fraction of surviving granules as a function of time, scaled with the estimated fitting parameter $a_{est,Ca}$ for the literature data sets from Suhairi [21]. Theoretically, all data should collapse onto the black curve e^{-t} .

In Figure 11, the effects of the poor prediction of the probability of breakage become clear. All silicone oil-based systems display more breakage than predicted. Particularly the systems using glass beads break much faster than anticipated. This may have to do with the particle shape and primary particle size as Equation 3 demonstrates, rounder particles result in weaker granules, and Akiti et al. [16] found that decreasing primary particle size reduces breakage;. The prediction in Equation 12 does not take this relationship into account. The breakage behaviour of systems closest to the test set, with silicone oil and lactose, show some agreement with the prediction, although the extent of breakage is still significantly underpredicted.

According to Figure 10, breakage is expected to be overpredicted for the water-based systems, as the model predicts a much higher probability of breakage than observed. However, as Figure 11 demonstrates, most of the water-based systems show such severe breakage that this overprediction does not matter; any sufficiently large number probability of breakage will follow the decay curve. In order to truly evaluate whether the model can predict the breakage behaviour of systems using different binders, such as water, much shorter granulation times are required; it is possible that the model still captures some of the breakage behaviour of such systems, as the capillary number does include some of the binder properties.

Overall, the obtained relationship presented in Equation 12 certainly gives a quantitative prediction of the breakage behaviour. However, a more detailed study is needed to properly account for the effect of other systems properties, such as powder-binder interactions and power properties. Furthermore, the current tests have only considered a single granulator design. By varying the design, it should be possible to provide predictions for r and s separately.

4 Conclusions

In this study, a model for predicting granule breakage in high-shear granulators has been developed. The model is based on the division of the granulator into a breakage zone, in which granules have a probability to break and a no-breakage zone, where no breakage occurs. The number of impacts, dependent on the granulation time, operating speed and the impeller shape, as well as the size of the breakage zone and the probability of granule breakage then determine the number of surviving granules.

A comparison with experimental data showed that the number of surviving granules does indeed decay exponentially, as predicted by the model. Relating the probability of breakage to the Stokes deformation number, St_{def} , which is associated with granule breakage, could not predict the number of surviving granules. Furthermore, the dimensionless peak flow stress, which is another measure of granule strength, was found to show only weak correlation with granule breakage. It was found that the inverse of the capillary number was linearly related to the probability of breakage. Moreover, the pore saturation was found to have a significant effect on the probability of breakage. The obtained relationship was used to predict the overall probability of breakage for all data sets evaluated. The resulting predictions agreed with the majority of the data sets evaluated.

A comparison with an experimental data set from Suhairi's work [21] showed that the predictions by the developed model agree qualitatively with the literature data, but the obtained relationship was not able to fully capture the breakage behaviour. This result can partially be attributed to the lack of early breakage data for systems that showed full breakage, as well as the use of a granules made using a single power-binder system to fit the model. The results demonstrate that the interaction between the powder and binder, as well as the powder

properties, may have a significant influence on the predictions. Currently, this influence is not captured by the proposed model.

This investigation into granule breakage has provided an interesting insight into the mechanisms and mechanistic modelling of breakage. For future work, an expanded set of data should be used to further explore the relationship between the capillary number, the pore saturation and the probability of breakage. Furthermore, attempts should be made to split the overall probability of breakage into the relative size of the breakage zone r and the actual probability of breakage s . In this way, it should be possible to account for changes in the size of the breakage zone caused by different impeller speeds. Additionally, by using granulators with varying dimensions and impeller shapes, the influence of the granulator configuration on the breakage zone can be inferred.

Nomenclature

Symbol	Name	Dimensions
a	lumped decay parameter	time ⁻¹
a_{Ca}	predicted lumped decay parameter using the capillary number	
a_{Str^*}	predicted lumped decay parameter using the dimensionless peak flow stress	
c_1	fitting constant for s	-
c_2	fitting constant for s	-
c_3	Fitting constant for s	time
AR	the shape factor of the primary particles	-
$d_{3,2}$	primary particle Sauter mean diameter	length
f	impeller shape factor	-
f_{Mat}	fracture behaviour of a particle	-
k	impact number	-
k_1	static strength of the granules	-
k_2	location of the transition from the static regime to the viscosity-dominated regime	-
N	the surviving number of granules	-

n	number of collision events	-
N_0	initial number of granules	-
r	relative granulator volume of the breakage zone	-
S	Liquid saturation	-
s	probability of breakage	-
St_{def}	Stokes deformation number	-
Str^*	dimensionless peak flow stress	-
t	granulation time	time
v_c	granule impact velocity	velocity
v_p	relative granule velocity	velocity
$W_{m,kin}$	kinetic energy of particle	energy
$W_{m,min}$	minimum kinetic energy required for particle breakage	energy
Greek Symbols		
γ	binder surface tension	pressure
ε	granule porosity	-
θ	powder-binder contact angle	degrees
μ	binder viscosity	pressure*time
ρ_g	granule density	density
σ_p	dynamic yield stress	pressure
ω	impeller speed	time ⁻¹
x	particle size	length

5 References

- [1] K. Hapgood, M. Rhodes, Size Enlargement, in: M. Rhodes, Editor, Introduction to Particle Technology, John Wiley & Sons Ltd., Chichester, 2008, pp. 337-358.
- [2] J. Litster, B.J. Ennis, L. Liu, The Science and Engineering of Granulation Processes, Kluwer Academic Publishers, Dordrecht, 2004.
- [3] D.M. Parikh, Introduction, in: D.M. Parikh, Editor, Handbook of Pharmaceutical Granulation Theory, Taylor & Francis Group, LLC, Boca Raton, 2005.
- [4] S.M. Iveson, J.D. Litster, K. Hapgood, B.J. Ennis, Nucleation, growth and breakage phenomena in agitated wet granulation processes: a review, Powder Technol. 117 (2001) 3-39.
- [5] A.D. Salman, G.K. Reynolds, H.S. Tan, I. Gabbott, M.J. Hounslow, Breakage in Granulation, in: A.D. Salman, M.J. Hounslow, and J.P.K. Seville, Editors, Handbook of Powder Technology, Elsevier Science B.V., 2007, pp. 979-1040.
- [6] R. Gokhale, Y. Sun, A.J. Shukla, High-Shear Granulation, in: D.M. Parikh, Editor, Handbook of Pharmaceutical Granulation Theory, Taylor & Francis Group, LLC, Boca Raton, 2005, pp. 191-228.
- [7] K.P. Hapgood, J.D. Litster, R. Smith, Nucleation regime map for liquid bound granules, AIChE J. 49 (2003) 350-361.

- [8] S.M. Iveson, J.D. Litster, Growth regime map for liquid-bound granules, *AICHE J.* 44 (1998) 1510-1518.
- [9] S.M. Iveson, P.A.L. Wauters, S. Forrest, J.D. Litster, G.M.H. Meesters, B. Scarlett, Growth regime map for liquid-bound granules: further development and experimental validation, *Powder Technol.* 117 (2001) 83-97.
- [10] P.C. Knight, T. Instone, J.M.K. Pearson, M.J. Hounslow, An investigation into the kinetics of liquid distribution and growth in high shear mixer agglomeration, *Powder Technology* 97 (1998) 246-257.
- [11] L. Vogel, W. Peukert, Characterisation of grinding-relevant particle properties by inverting a population balance model, *Particle & Particle Systems Characterization* 19 (2002) 149-157.
- [12] K. van den Dries, O.M. de Vegt, V. Girard, H. Vromans, Granule breakage phenomena in a high shear mixer; influence of process and formulation variables and consequences on granule homogeneity, *Powder Technology* 133 (2003) 228-236.
- [13] G.I. Tardos, M.I. Khan, P.R. Mort, Critical parameters and limiting conditions in binder granulation of fine powders, *Powder Technology* 94 (1997) 245-258.
- [14] L.X. Liu, R. Smith, J.D. Litster, Wet granule breakage in a breakage only high-shear mixer: Effect of formulation properties on breakage behaviour, *Powder Technology* 189 (2009) 158-164.
- [15] R.M. Smith, L.A.X. Liu, J.D. Litster, Breakage of drop nucleated granules in a breakage only high shear mixer, *Chemical Engineering Science* 65 (2010) 5651-5657.
- [16] N. Akiti, Y.S. Cheong, K.P. Hapgood, D. Khakhar, A study of wet granule breakage in a breakage-only high-shear mixer, *Advanced Powder Technology* 31 (2020) 2438-2446.
- [17] S.A.L. De Koster, *Experimental investigation and modelling of consolidation and layering mechanisms in high-shear granulation*. 2018, University of Sheffield: Sheffield.
- [18] R.M. Smith, J.D. Litster, Examining the failure modes of wet granular materials using dynamic diametrical compression, *Powder Technology* 224 (2012) 189-195.
- [19] S.M. Iveson, J.A. Beathe, N.W. Page, The dynamic strength of partially saturated powder compacts: the effect of liquid properties, *Powder Technology* 127 (2002) 149-161.
- [20] S.M. Iveson, N.W. Page, Dynamic strength of liquid-bound granular materials: The effect of particle size and shape, *Powder Technology* 152 (2005) 79-89.
- [21] N.N. Suhairi, *Wet Granule Breakage in a High Shear Mixer*, in *Faculty of Engineering, Physical Sciences, and Architecture*. 2006, The University of Queensland: Queensland.